HHS Public Access

Author manuscript

Nat Rev Bioeng. Author manuscript; available in PMC 2024 March 01.

Published in final edited form as:

Nat Rev Bioeng. 2023 September ; 1(9): 617–630. doi:10.1038/s44222-023-00086-w.

Brain imaging with portable low-field MRI

W. Taylor Kimberly[1], **Annabel J. Sorby-Adams**[1], **Andrew G. Webb**[2], **Ed X. Wu**[3], **Rachel Beekman**[4], **Ritvij Bowry**[5], **Steven J. Schiff**[6], **Adam de Havenon**[7], **Francis X. Shen**[8,9], **Gordon Sze**[10], **Pamela Schaefer**[11], **Juan Eugenio Iglesias**[12,13,14], **Matthew S. Rosen**[12], **Kevin N. Sheth**[4]

[1]Department of Neurology and the Center for Genomic Medicine, Massachusetts General Hospital and Harvard Medical School, Boston, MA, USA.

[2]Department of Radiology, Leiden University Medical Center, Leiden, The Netherlands.

[3]Laboratory of Biomedical Imaging and Signal Processing, Department of Electrical and Electronic Engineering, The University of Hong Kong, Hong Kong SAR, China.

[4]Division of Neurocritical Care and Emergency Neurology, Department of Neurology, Yale New Haven Hospital and Yale School of Medicine, Yale Center for Brain & Mind Health, New Haven, CT, USA.

[5]Departments of Neurosurgery and Neurology, McGovern Medical School, University of Texas Health Neurosciences, Houston, TX, USA.

[6]Department of Neurosurgery, Yale School of Medicine, New Haven, CT, USA.

[7]Division of Vascular Neurology, Department of Neurology, Yale New Haven Hospital and Yale School of Medicine, New Haven, CT, USA.

[8]Harvard Medical School Center for Bioethics, Harvard law School, Boston, MA, USA.

[9]Department of Psychiatry, Massachusetts General Hospital, Boston, MA, USA.

[10]Department of Radiology, Yale New Haven Hospital and Yale School of Medicine, New Haven, CT, USA.

[11]Division of Neuroradiology, Department of Radiology, Massachusetts General Hospital and Harvard Medical School, Boston, MA, USA.

[12]Athinoula A. Martinos Center for Biomedical Imaging, Department of Radiology, Massachusetts General Hospital and Harvard Medical School, Boston, MA, USA.

[13]Centre for Medical Image Computing, University College London, London, UK.

[14]Computer Science and AI Laboratory, Massachusetts Institute of Technology, Boston, MA, USA.

wtkimberly@mgh.harvard.edu; kevin.sheth@yale.edu.

Author contributions

All authors contributed to the planning, drafting and editing of this Review.

Competing interests

M.S.R. is a founder and equity holder of Hyperfine Inc. W.T.K. and K.N.S. have sponsored research agreements between their respective institutions and Hyperfine Inc. All other co-authors declare no conflict of interest.

Abstract

The advent of portable, low-field MRI (LF-MRI) heralds new opportunities in neuroimaging. Low power requirements and transportability have enabled scanning outside the controlled environment of a conventional MRI suite, enhancing access to neuroimaging for indications that are not well suited to existing technologies. Maximizing the information extracted from the reduced signal-to-noise ratio of LF-MRI is crucial to developing clinically useful diagnostic images. Progress in electromagnetic noise cancellation and machine learning reconstruction algorithms from sparse *k*-space data as well as new approaches to image enhancement have now enabled these advancements. Coupling technological innovation with bedside imaging creates new prospects in visualizing the healthy brain and detecting acute and chronic pathological changes. Ongoing development of hardware, improvements in pulse sequences and image reconstruction, and validation of clinical utility will continue to accelerate this field. As further innovation occurs, portable LF-MRI will facilitate the democratization of MRI and create new applications not previously feasible with conventional systems.

Introduction

The origin of neuroimaging dates to the turn of the twentieth century when X-rays were first discovered and used to image the skull[1,2]. It was not until three-quarters of a century later that computerized tomography (CT) scanning led to the first non-invasive three-dimensional (3D) images of the brain and its substructures[3,4]. Shortly thereafter, in vivo NMR detection of water protons was combined with spatial encoding using magnetic field gradients to enable the first MR images of the brain[5,6]. Over the ensuing decades, improvements in resolution, contrast and image reconstruction have reinforced these techniques as central to neurological, neurosurgical and neuroscientific investigation. Collectively, CT and MRI modalities have transformed our understanding of the brain in both normal and pathological states.

From a diagnostic perspective, present-day neuroradiological examination is paramount to the evaluation and management of numerous neurological diseases, including stroke, intracranial haemorrhage, brain tumours, multiple sclerosis (MS), dementia and hydrocephalus. The choice of CT versus MRI represents trade-offs between diagnostic sensitivity and specificity, safety, cost, and accessibility. For MRI, the clinical imperative for shortened scan times and increased resolution that accompanies the improved signal-to-noise ratio (SNR) has focused most technological developments toward increasing the strength of the main magnetic field (termed B_0). However, higher magnetic field strengths necessitate supercooling cryogens, high power and electrical current requirements, and specialized safety protocols for addressing thermal heating, acoustic noise and ferromagnetic materials. Collectively, these features require a large initial capital investment in machinery, with substantial operational costs, which has the overall consequence of reduced accessibility of MRI. However, not every diagnostic question requires high-resolution imaging; therefore, MRI devices with lower magnetic field strength and lower image resolution have the potential to fill an important niche owing to lower cost and increased access. In this context, lower field strength represents engineering innovation, whereas portability and lower cost

represent public health innovation. Taken together, accessible and affordable low-field MRI has the potential for high impact at the population level if implemented appropriately.

MRI scanner design involves choices with respect to field strength, magnet type, scanner geometry and instrument citing. For the purpose of this Review, MRI scanners operating with a primary magnetic field strength between >10mT and ≤100mT are termed low-field MRI (LF-MRI), whereas those operating between >100mT and ≤1.0 T are mid-field MRI, >1.0 T and ≤3.0 T are high-field MRI (HF-MRI), and >3.0 T are ultra-high-field MRI. Scanners operating below 10 mT are known as ultra-low-field MRI. The majority of clinical scanners correspond to HF-MRI, where the average superconducting magnet weighs 4,500–7,500 kg and requires fixed housing in a dedicated MRI suite with an adjacent control room and separate access for cryogenic components. Patients must therefore be physically transported to a centralized diagnostic MRI suite to undergo imaging.

By contrast, scanners with magnetic field strengths in the LF range are generally built using permanent magnets, which avoids the need for supercooling cryogens and reduces power consumption. Relative to superconducting electromagnets, which are typically arranged in a cylindrical bore configuration, permanent magnet scanners are typically constructed using C-arm, H-arm or Halbach array geometries[7]. Collectively, the choice of magnet, its electrical power requirements and the associated geometry have a major impact on siting constraints, which range from access-controlled, fixed locations to portable scanners that are compatible with imaging adjacent to nearby ferromagnetic materials. For this Review, portable MRI refers to fully self-contained devices with the ability to move to the bedside for imaging acquisition or to scanners located within a mobile vehicle enabling imaging within the community. Although not all LF-MRI systems are transportable (for example, a fixed location LF system), many of the features that define LF-MRI enable this class of scanners to be portable. For LF-MRI devices, the main limitation is the lower SNR leading to reduced image resolution and longer acquisition times. However, recent advances in hardware and software for LF-MRI have unlocked the strength of this area as a promising option for both clinical diagnostic and scientific questions. The summary of those advances and clinical applications is the focus of this Review.

Hardware and software requirements

Although the detailed physics and principles underpinning MRI are beyond the scope of this Review, there are several features and concepts that are essential in MR system design. The B_0 field (typically measured in Tesla) creates a Boltzmann distribution of nuclear spin alignment (known as polarization) in hydrogen-containing tissues, primarily water and lipid. The inductive detection of this nuclear polarization forms the signal in proton MRI. The magnet is designed such that the B_0 field is as homogenous as possible to perform high-resolution imaging. So-called shim coils are used to further improve the homogeneity of the main B_0 field for individual people being scanned.

To spatially encode the MR signal, computer control of the current passing through magnetic field gradient coils is used to phase-modulate and frequency-modulate the detected MR signal. The gradient coils are securely fixed inside the magnet. Radiofrequency (RF) coils

are used to transmit a RF pulse at the proton resonance frequency and to detect the precessing nuclear spin magnetization. The phase-encoded and frequency-encoded data can be represented in the *k*-space or spatial frequency domain. Reconstruction of the image in the spatial domain involves inverting the forward encoding model, which, for standard Cartesian *k*-space imaging, is a simple inverse Fourier transform. Other more sophisticated reconstruction approaches are used for non-Cartesian acquisition strategies, such as spiral and radial sampling, and for acquisitions that undersample *k*-space. The spatial resolution and overall quality of the reconstructed image ultimately depend on the SNR of the acquired data, which is much lower in LF-MRI systems than for conventional HF counterparts.

Several bioengineering advances in LF-MRI hardware and software have enabled the realization of portable MRI in the clinical environment. Below, we summarize some of those developments and highlight new directions.

Hardware considerations

From a hardware perspective, there are several important considerations that are crucial to enabling portability for a LF-MRI system. These factors include a reasonable weight and size, a tight fringe field that limits the extent of the peripheral magnetic field, power requirements that can be supplied by standard electrical outlets, no active cooling, built-in shielding and/or RF interference cancellation, and low acoustic noise. Together, these features facilitate portability, both through the incorporation of wheels and motors in device design enabling transportation by a single operator, and in siting scanners outside of access-controlled environments such as in mobile vehicles. In addition, the primary magnet must have sufficient homogeneity of the B_0 field to facilitate acceptable spatial resolution and geometric accuracy as well as a field strength that is high enough for sufficient SNR.

For portable systems, the use of permanent magnets has emerged as a means to mitigate the electric power and cooling needs of resistive electromagnets (for recent resistive electromagnet development, see refs.[8–11]). Permanent magnets are comprised of either neodymium–iron–boron (NdFeB) or samarium–cobalt (SmCo). NdFeB gives a higher field strength than SmCo but field drift is more temperature dependent. There are two main geometries used to generate the B_0 field: a Hal-bach array or planar magnets in a C-shape or H-shape. C-shaped and H-shaped magnets consist of two large discs, and the patient is positioned between them. The two magnets are connected through either a single (C-shaped) or two (H-shaped) ferromagnetic yokes (Fig. 1). C-shaped and H-shaped geometries have weights on the order of 350– 450 kg, field strengths of 50–64 mT and B_0 field homogeneities of ~250–500 parts per million (ppm) after shimming[12–14]. In comparison, Halbach array[15] permanent magnet systems employ several small magnets[7,16,17] that are arranged to give either a homogeneous magnetic field or one with an in-built gradient[16,18–21] (Fig. 1). Typical weights for Halbach arrays are lower than planar disc geometries with weights of 35–70 kg, field strengths of 50–80 mT and a B_0 field homogeneity of ~1,000 ppm after shimming.

Gradient coil designs depend largely on magnet geometry; for C-shaped and H-shaped magnets, planar gradient coils[22] on each pole piece are used[23–26], for Halbach arrays, the gradient coils are arranged in a cylindrical geometry[20,27]. In general, both systems have

much lower acoustic noise levels than HF-MRI owing to reduced Lorentz forces, which are the combined electric and magnetic force on a point charge that is due to the electromagnetic field[28]. Lorentz forces are used to create vibrations in the gradient coils yet they can also cause acoustic noise. Gradient amplifiers for portable MRI, which may be commercial or custom-built, produce peak currents of between ~30 and 150 amps.

Taken together, there are trade-offs for each type of magnet design. For example, planar disc designs are simpler to construct, are more open and typically have better B_0 field homogeneity. However, they tend to have greater mass and the planar gradient coils used are intrinsically less efficient. Conversely, Halbach arrays with a cylindrical geometry produce the maximum field strength per unit weight of magnetic material and are consequently lighter. These systems also have more efficient cylindrical gradient coils but the greater B_0 field inhomogeneities can adversely impact spatial resolution. Strategies have been proposed that eliminate one or more gradient coils from the scanner in lieu of using an inherent 'built-in' static magnetic gradient[18] to perform spatial encoding or by using RF-encoding strategies such as Transmit Array Spatial Encoding[19,29–31].

Key to the operation of MR systems is the ability to transmit resonant RF pulses to excite the nuclear spins in the imaging volume and to receive the weak signal arising from precessing nuclear magnetization. These transmit and receive systems are essentially antennas that are tuned for operation at the appropriate Larmor frequency, which is 42 MHz/T (42 kHz/mT) for proton (water) imaging. These antennas are known colloquially in the MRI RF engineering community simply as the 'RF coil'. The direction of the magnetic field (termed B_1) produced by these RF coils must be oriented perpendicular to the axis of the B_0 field. RF coils for MR have been reviewed in detail elsewhere[32].

Each of the LF magnet geometries described above produces a B_0 field oriented transverse to the patient axis, with two possible perpendicular directions for the B_1 field direction. For adult neuroimaging, an outer cylindrical solenoid transmit coil and an inner elliptical solenoid coil for signal reception can be used[12,14]. Quadrature receive coils have also been developed[33]. Moreover, an elliptical spiral solenoid[11] has been constructed to conform tightly with the human head for both transmission and reception[20,34]: the B_1 field uniformity can be optimized using a variable winding pitch[35]. Images have also been obtained[18,36] from multi-element receive coil arrays like those on a commercial portable LF-MRI system[13]. Both custom-built and commercial RF amplifiers have been used on portable LF-MRI systems, with outputs on the order of tens of Watts required.

In terms of future hardware developments, new design techniques, such as those based on artificial intelligence (AI)[37], may lead to lighter, stronger and more homogeneous magnet designs. Many LF systems use RF coils wound with standard copper wire and have a reduced quality factor owing to the ratio between the central frequency and the bandwidth[32]. The use of Litz wire[11,35,38] to increase the coil quality factor is a strategy to reduce detector noise. Ultra-low-noise, 50-Ω RF preamps suitable for operation at the LF and ultra-low-field Larmor frequencies have also become available, which can be used to obtain a lower receiver noise floor. Especially in the case of highly inhomogeneous magnets, the RF coil bandwidth might become too narrow to accommodate the necessary imaging

read-out bandwidth. In these cases, the use of impedance-mismatched preamplifiers to expand the receive bandwidth could be used. Even more compact systems can be designed when full imaging capability is not needed such as to obtain spectroscopic or relaxometric information. Such systems rely on single-sided MR[39–41].

Electromagnetic interference

For MRI scanners with a fixed siting, ambient electromagnetic noise can be shielded from the instrument by constructing a conductive enclosure around the scanner suite (that is, a Faraday cage). For portable systems, an alternative solution is needed to manage electromagnetic interference (EMI)[14,42].

Several active EMI cancellation methods have been recently developed to remove EMI for LF-MRI without requiring an RF-shielded room. An analytical approach was proposed to estimate the EMI signal in the MRI receive coil from EMI signals detected by EMI sensing coils based on the frequency domain transfer functions among coils[43]. This strategy was later extended for time domain implementation as linear convolutions and with an adaptive procedure[42]. A commercially available FDA-cleared 0.064 T brain MRI scanner can operate in unshielded environments using an EMI removal method, which was first described in 2017 (ref.44) and further described more recently[13,45,46]. A deep learning approach was also developed to derive a more accurate model to predict the EMI signal in an MRI receive coil from the EMI signals detected by EMI sensing coils[14,47]. In general, these methods take advantage of the well-established multi-receiver MRI electronics previously developed for parallel imaging. They are also underpinned by a simple electromagnetic phenomenon; that is, the properties of RF signal propagations among any radiative (for example, air) or conductive media (for example, surrounding EMI-emitting structures such as power lines, RF coils, other MRI hardware pieces and cables, or patient monitoring equipment) are fully dictated by the electromagnetic coupling among these media or structures. Such coupling relationships can be analytically characterized in a simple manner by the frequency domain coupling or transfer functions among structures (for example, among MRI receive coil and sensing coils). In turn, this information can be used to estimate the EMI signal and remove it from the reconstructed image.

The ideal EMI cancellation method must handle EMI signals that change dynamically over time during MRI scanning. Such changes can arise from the surrounding EMI sources that demonstrate different behaviours. EMI signals received by MRI receive coils can also be influenced by the human body, which serves as an antenna[48,49] for EMI reception in a shielding-free MRI setting. For example, varying body size and weight can alter the level and characteristics of EMI signals picked up by the body and subsequently detected by the MRI receive coil. Changes in human body position during MRI scanning can also alter the EMI signal detected by the MRI receive coil owing to alterations in electromagnetic coupling between surrounding EMI-emitting sources and the receiving human body. Consequently, adaptive approaches[50,51] that rely on deep learning are found to be more effective in practice. Future development should focus on robust cancellation methods in the presence of strong and complex EMI environments.

Pulse sequence and data acquisition

Although numerous MRI protocols have been developed since the 1980s, the most valuable and universally adopted neuroimaging protocols are T1-weighted (T1W) imaging, T2-weighted (T2W) imaging, fluid-attenuated inversion recovery (FLAIR), diffusion-weighted imaging (DWI) and susceptibility-weighted imaging (SWI)[52]. T1W images rely on the longitudinal relaxation of proton spins to generate tissue contrast, whereas T2W contrast is based on the transverse relaxation of spinning protons. FLAIR is a T2W image with an inversion pulse implemented to suppress the signal from cerebrospinal fluid (CSF). DWI generates images based on differences in Brownian motion. SWI is a gradient-echo-based sequence that is sensitive to small magnetic field inhomogeneities, making it susceptible to ferromagnetic materials. At LF, T1W protocols can be implemented using 3D gradient-echo[12,14,34] or 3D fast-spin-echo (FSE) with inversion preparation[13,20,45], whereas T2W protocols are commonly implemented using 3D FSE sequences[13,14,20,45]. A FLAIR protocol can be achieved through either a traditional inversion-prepared 3D FSE sequence[13,45] or a simple short repetition time 3D FSE sequence[14].

DWI is technically more challenging at LF but remains a clinically valuable protocol, particularly for early stroke diagnosis. Strong diffusion gradients make DWI intrinsically sensitive to patient motion and are also hardware demanding. Although 2D FSE and 3D steady-state gradient-echo sequences have been attempted[13,45], single-shot 2D echo-planar-imaging sequences generate more reproducible brain DWI results owing to relative motion insensitivity[14]. Given that T1 values of various tissues are generally much shorter at LF[53] (with the exception of CSF), direct 3D DWI protocols with short repetition time are desirable. DWI protocols on current FDA-approved LF-MRI devices are limited to acquisition in a single diffusion direction and do not use multiple *b*-values (protocols limited to $b = 0$ and $b = 900$ s/mm^2). A *b*-value is a measure of the strength of the diffusion gradients applied during a scan. Higher *b*-values can improve the sensitivity of the scan in detecting water diffusion but can also reduce image quality. Expanding the capabilities of DWI with isotropic diffusion weighting and high-SNR in addition to improving image quality against hardware imperfections are avenues for ongoing development. Implementation of SWI and other sequences that rely on magnetic susceptibility, such as blood oxygen-dependent imaging, is challenging at LF owing to low magnetic susceptibility. As with DWI, this remains an area for future research. In parallel, alternative data acquisition and reconstruction methods, such as TrueFISP-based MR fingerprinting[54] or deep learning reconstruction[55–57], have been used to boost the attainable image quality from low SNR or incomplete 3D *k*-space data acquired at LF[58,59].

Machine learning and AI

Even with further improvement in hardware and software at LF, there is currently a sizeable gap in image quality between the reconstructed LF images when compared side-by-side to HF-MRI (Fig. 2). One emerging strategy to narrow this gap is to develop super-resolution methods, that is, techniques that increase the resolution of an imaging system. Such techniques have the potential to synthesize a high-resolution image from a lower-resolution LF counterpart.

Early super-resolution methods were developed for photography and capitalized on multiple images from the same scene (with sub-pixel shifts) to estimate a higher-resolution image. These methods were superseded by single-image methods, where machine learning techniques are used to predict a high-resolution image from a low-resolution input. These methods are typically trained in a supervised fashion, that is, 'teaching' the method with numerous pairs of low-resolution and high-resolution images of the same scene. State-of-the-art super-resolution follows this paradigm, using modern AI techniques based on convolutional neural networks (CNNs)[60]. The most successful CNNs are trained in a supervised fashion with a large pool of paired, spatially aligned high-resolution and low-resolution images to estimate a mapping between the two[61–63]. Unsupervised strategies using perceptual losses based on adversarial networks[64] also exist and do not require paired images: by fooling a discriminator trained to differentiate super-resolved and real high-resolution images, the properties of high-resolution images can be learned. However, adversarial perceptual losses are normally used in conjunction with supervised methods to improve the accuracy of the synthetic images as they underperform when used in isolation[65].

Paired data to train super-resolution CNNs for portable LF-MRI will become available with time yet data are currently limited. Even with the compilation of large data sets of paired HF and LF images from the same individuals, spatial alignment is a challenge between the two field-strength images. Estimating this alignment with deformable image registration[66] is difficult owing to the large differences in non-linear spatial distortion and resolution. An alternative approach is to artificially down-sample HF-MRI scans (whereby images are reduced in spatial resolution) to obtain pairs of images that are perfectly aligned by construction but are limited, a problem known as 'domain shift'[67]. Alternative strategies, such as domain adaptation techniques[68], unsupervised techniques or domain randomization techniques[69,70], may eventually bridge this domain gap and reach a level of performance that is not far behind that of supervised methods.

A crucial component of these AI strategies will be the ability to quantify the uncertainty of the predictions. Neural networks can hallucinate features in image regression problems, particularly when using adversaries[71]. Therefore, knowing when and where a prediction is likely to be wrong is of great importance in clinical settings. This requires estimating two sources of uncertainty: aleatoric and epistemic. The former is dependent on input and can be learned from training data with statistical distributions; the latter is in the CNN weights. Advances in areas such as prior networks[72], Bayesian deep learning[73], Monte Carlo dropout[74], deep ensembles[75] or evidential deep learning[76] could provide the rigorous uncertainty estimation that will be required for clinical applications.

Another critical aspect of AI systems is the potential presence of biases in the trained systems ('AI safety'). Such biases are almost always the product of a lack of diversity in the training data[77] and are known to be possibly very large in image classification CNNs operating at the global level. For example, error rate increases have been found in under-represented groups in Alzheimer disease classification[78] following previous results from the non-medical literature (for example, recidivism prediction[79,80] or childhood welfare[81]). To the best of our knowledge, the effect of AI biases on super-resolution has never been specifically studied. Being a voxel-wise regression problem, where predictions are made

semi-locally, AI biases should be less problematic than in image classification. However, mild group-wise differences in performance have been found in other voxel-wise tasks such as image segmentation of cardiac and brain MRI[82,83]. Therefore, we believe that it will be of paramount importance to study the presence of biases in AI-enabled super-resolution of LF-MRI before deployment as well as to assess the effectiveness of existing bias mitigation approaches[84], possibly developing new mitigation strategies that are specific to this imaging domain. Such studies will require the acquisition and curation of diverse paired LF-MRI and HF-MRI data sets.

Clinical applications

With recent advances in LF-MRI scanners that are approved by the FDA for clinical use, imaging at LF is starting to be evaluated in inpatient hospital environments and community-based settings (Fig. 2). Here, we summarize some of the emerging experiences of applying LF-MRI in these areas.

Stroke and intracerebral haemorrhage

Timely neuroradiological examination is a crucial step in the diagnosis and management of stroke. Current guidelines recommend that patients with suspected stroke receive emergency imaging on hospital arrival to differentiate acute ischaemic stroke (AIS) from intracerebral haemorrhage (ICH). Traditionally, neuroimaging for stroke has been performed using non-contrast CT or MRI, with the former being the imaging modality of choice owing to better accessibility at most primary stroke centres. For AIS, a head-to-head trial of MRI versus CT demonstrated that MRI was superior to CT for the diagnosis of acute infarction[85], with a higher sensitivity especially in the first 6 h after stroke onset and for the detection of small infarcts[85–87]. DWI detects the reduced diffusion of water that occurs within minutes of ischaemia onset[88], and the interpretation of DWI is reliable among readers with different levels of experience[89].

Multimodal MRI has also been shown to improve patient selection procedures for thrombolysis treatment. For example, in the setting of stroke with an unknown time of onset (often termed wake-up stroke), DWI and FLAIR imaging can be used to estimate the time of stroke onset and guide treatment with tissue plasminogen activator[90–92]. In the evaluation of ICH, non-contrast CT has a high sensitivity to blood products and has historically been the imaging modality of choice. However, multimodal MRI has been shown to be as accurate as CT in detecting ICH, improving classification of extra-axial haemorrhage while circumventing exposure to CT radiation[93]. Nevertheless, timely access remains a barrier to implementing MRI in patient diagnosis and treatment selection procedures, with many centres continuing to favour CT owing to acquisition times and cost efficiencies.

LF-MRI offers a unique potential for stroke diagnosis and intervention. LF-MRI can detect both AIS and ICH; specifically, it was able to detect diffusion restriction in 45 out of 50 (90%) patients with acute ischaemic stroke identified on HF-MRI[94]. Moreover, in 144 patients with ICH or AIS compared with healthy controls, the sensitivity and specificity for detection of ICH was high (sensitivity 80.4%, specificity 96%)[95]. However, as the majority of reported acquisitions were performed in the subacute time frame, systematic

hyperacute imaging and head-to-head comparisons with current modalities is needed. In addition, real-time interpretation across a range of readers needs to be evaluated to optimize routine real-world use.

Portable LF-MRI could also expedite stroke diagnosis across a range of environments, including those previously unable to support conventional HF-MRI. This encompasses small community hospitals in remote areas, planes, ambulances and emergency departments. Mobile stroke ambulances with onboard CT scanners have already shown benefit, including improved patient outcomes and reduced disability[96]. Ambulances with onboard LF-MRI scanners could also hold considerable potential, particularly in advancing the diagnosis and treatment of patients with acute stroke using multimodal imaging.

Cardiac arrest and critical care

In addition to imaging stroke and its complications, portable LF-MRI has been used to monitor for neurological complications in critically ill populations. Despite the diagnostic value of imaging critically ill patients, transport out of the intensive care unit (ICU) to centralized imaging suites is not always feasible owing to the risk for life-threatening haemo-dynamic, respiratory and/or neurological adverse outcomes[97–100]. As a result, gaps in information conferred by MRI can occur, which are pivotal for clinical decision-making[101–104].

LF-MRI is safe and feasible to perform in critically ill patients[13], including those who have been traditionally excluded from neuroimaging[13,105,106]. LF-MRI imaging has also been acquired in patients undergoing extracorporeal membrane oxygenation, including for the detection of previously unsuspected strokes[106]. In a cohort of patients with severe acute respiratory distress syndrome related to COVID-19, with unexplained encephalopathy, seizures, focal neurological deficit or an abnormal head CT, 12 (63.2%) patients had abnormal findings on LF-MRI. These findings included increased FLAIR signal, cerebral haemorrhage and diffusion restriction on DWI. Although abnormal findings changed management in 5 (41.6%) patients, normal MRI allowed providers to adjust the differential diagnosis or provide reassurance when discussing goals of care[107]. Similarly, in a cohort of 20 patients with altered mental status and COVID-19, portable LF-MRI identified abnormalities in 8 (40%) patients[13].

Survivors of cardiac arrest are another critically ill population at high risk for travel out of the ICU. HF-MRI is more sensitive than CT for the detection of hypoxic–ischaemic brain injury and provides information for neurological prognostication[108,109]. An initial experience in imaging cardiac arrest survivors with LF-MRI established that imaging could occur without interruption of continuous haemodynamic monitoring or disruption of targeted temperature management. Portable LF-MRI exams managed to detect the same hypoxic–ischaemic injury that was detected on conventional neuroimaging earlier than conventional HF-MRI by approximately 33 h (ref.105).

Paediatric brain development

Neuroimaging is playing an increasing role in understanding neurodevelopment in children. Growth charting is central to paediatric care, and ongoing efforts have sought to extend these

normative charts to the developing brain. For example, percentile brain growth charts for children with normal development have been constructed, and an age-dependent universal ratio of brain-to-CSF volume, independent of sex or anthropometric body size, has been observed[110]. Furthermore, brain volume across the lifespan has also been explored with utility beyond childhood[111]. Observing and optimizing brain growth requires automated segmentation of images obtained using MRI, and quantifying both brain and CSF volume as a function of age is showing increasing value[112]. Access to conventional MRI as a serial screening tool for such purposes is limited. However, paediatric LF-MRI neuro-imaging in children aged 6 weeks to 16 years has been performed, with volumetric results obtained on LF-MRI compared to conventional 3 T counterparts[113]. Although confidence intervals were substantially broader at LF, preliminary findings in 42 children reported strong agreement between developmental trajectories calculated on both LF-MRI and HF-MRI[113].

LF-MRI also has potential in the setting of the neonatal ICU (NICU), where brain imaging is used to diagnose and monitor conditions such as hypoxic–ischaemic injury, haemorrhage and congenital brain malformations. Comparable to the adult ICU, conventional HF-MRI is not compatible with NICU support equipment, including incubators and monitors, and despite efforts to develop MR-compatible devices[114,115], movement of critically ill infants to centralized imaging suites remains an important clinical concern[116]. Furthermore, one of the most notable contraindications to paediatric MR is motion artefact, with infants often requiring anaesthesia or sedation to tolerate the exam, albeit at an increased risk to the patient[117,118]. Approaches to circumvent sedation include scanning infants during sleep, in the evening, or following feeding or swaddling. LF-MRI enables imaging at the bedside and in the presence of ferromagnetic equipment, where the lower acoustic noise of LF-MRI systems facilitates movement of children into the scanner while enabling staff or caregivers to maintain physical contact during the exam owing to the reduced fringe field[113].

LF approaches also allow for the development of specific magnet geometries for imaging the neonatal brain, with several systems designed specifically for infant populations[8,118]. To facilitate NICU scanning, early investigations involved a 0.17 T system deployed in the United Kingdom, enabling imaging of infants aged approximately 16.3 days, including 43 with suspected pathology[118]. Subsequently, a 0.064 T system was deployed in a NICU, enabling 14 neonates with an average age of 29.7 days to be imaged[116]. LF-MRI was able to detect notable pathology, although subtle pathology was missed, likely caused by the low SNR and resolution, especially for findings on DWI and T1. Despite benefits of LF-MRI in the NICU, image quality remains a barrier to post-processing (such as skull stripping) and subsequent interpretation. Additional assessment of the usefulness of LF-MRI imaging in the paediatric population and the impact on patient outcome is an avenue for future research.

Beyond the NICU, the value of paediatric LF-MRI imaging in low-income and middle-income countries is of relevance, especially for the detection of hydrocephalus. Hydrocephalus predominantly arises because of infection, haemorrhage or other inflammatory conditions[119], and is the most common indication for neurological surgery for children. In industrialized countries, the primary cause is intraventricular haemorrhage of prematurity. In the developing world, infection early in life, often in survivors of neonatal

sepsis[120], is the predominant cause[120,121], with the prevalence of hydrocephalus in these regions vastly exceeding that in industrialized countries.

Neuroimaging is not only useful for the diagnosis of hydrocephalus but is necessary for treatment and continued management. Because growth arrest of the brain can occur in untreated hydrocephalus and catch-up growth has followed treatment and pressure relief[122], early detection and surgical intervention are needed to minimize the impact on long-term brain growth patterns[123]. This can be achieved with different modalities, including MRI, CT or ultrasound. Ultrasound can image hydrocephalus configurations within the brain but only in the youngest infants when acoustic windows through open fontanelles are still available. CT scanning is an alternative but has attendant concerns for the potential carcinogenic risks of ionizing radiation, particularly from early exposures in infancy[124]. HF-MRI avoids the risk of ionizing radiation but is too expensive and complex to maintain in many medical systems where paediatric hydrocephalus is most prevalent. CSF diversion interventions guided by neuroimaging are enabled through segmentation of brain tissue and CSF spaces. These include traditional ventriculoperitoneal shunt systems and, more recently, endoscopic fenestration within the brain to re-establish CSF flow[122]. In both scenarios, neuroimaging is necessary to assess the adequacy of fluid management and monitor for complications such as overdrainage[125]. LF-MRI holds the potential to extend adequate treatment and management of hydrocephalus to patients in all regions of the world. Despite the inherently lower resolution and tissue contrast of LF-MRI, it could provide adequate assessment of ventricular spaces both before and after hydrocephalus interventions. This comparison has been investigated in degraded hydrocephalic images of young children, and the clinical utility of lower-quality images has been explored[126].

Beyond paediatric neuroimaging, LF-MRI has great potential in enhancing access to MRI in resource-constrained countries where CT or HF-MRI are lacking (Box 1).

Chronic neurological diseases

The diagnosis and subsequent management of chronic neurological and neurodegenerative diseases is frequently guided by neuroimaging. MRI enables segmentation of cortical regions and determination of morphological changes, which can be indicative of neurodegenerative disease progression. However, the undiagnosed burden of neurological disease remains a crucial barrier to improving brain health at a population level. Depending on the patient population, relevant and potentially modifiable asymptomatic neurological disease can be found in up to 20–30% of individuals[127–132].

Although MRI of the brain is an effective method of screening for asymptomatic neurological disease, expense and logistical complexity have limited large-scale screening efforts. Furthermore, conventional screening efforts often fail to reach underserved populations who would most benefit from screening and pre-emptive care[133,134]. Potential use-case scenarios for chronic neurological disease monitoring includes cerebral small vessel disease, which leads to white matter hyperintensities (WMH), a subclinical brain pathology prevalent in over half of community-based adults above 60 years of age[135–138]. Neuroimaging-ascertained WMH are a highly prevalent vascular risk factor for cognitive decline, cardiovascular disease and stroke[139–141], and early detection and modification

through improved blood pressure control can reduce WMH progression[142–145]. In a diverse cohort of 91 individuals scanned in an emergency department patient room, 74% had prevalent hypertension and 58% were found to have moderate-to-severe WMH on bedside LF-MRI[146]. Most individuals had not otherwise had an MRI in the preceding year. Future studies should examine the role of WMH in the community setting and the potential role of LF-MRI in reducing known disparities in neuroimaging[147].

Similarly, neurodegeneration caused by Alzheimer disease leads to brain atrophy that can be used to assist in the diagnosis and monitoring of disease progression. Serial HF-MRI is impractical for most patients owing to the cost and complexity; however, a portable LF-MRI system sited in an outpatient clinic could obtain serial images to assess change over time. Nevertheless, the native lower-resolution images from LF-MRI might require additional image enhancement, such as super-resolution, to achieve reliable segmentation volumes[69]. As targeted Alzheimer disease treatments emerge on the therapeutic horizon, it will be important to validate, in broad and diverse populations, imaging biomarkers to track responsiveness to treatment or adverse treatment effects such as brain inflammation from amyloid-modifying therapy.

Another example is the monitoring of chronic neurological diseases such as demyelination observed in MS. The feasibility of LF-MRI for the identification of MS demyelinative lesions has been examined in a cohort of 33 patients, whereby lesions were correctly identified in 31 (94%) individuals. The smallest lesions detected measured 5.7 mm, with a high correlation between lesion volume quantified on both LF-MRI and conventional HF-MRI ($r = 0.89$; $P < 0.001$)[148,149].

LF-MRI of the brain thus has multiple potential applications in the care of individuals with chronic neurological disease. Furthermore, LF-MRI could enable the evaluation of individuals at a scale that could not be accomplished using conventional MRI alone. Because portable LF-MRI can be transported within a health-care facility or with a dedicated vehicle between facilities[150], it would be feasible to scan individuals at the point of care, reducing disparities in access to diagnostic imaging[147,151–154].

Outlook

Portable LF-MRI has demonstrated potential in the management of neurological and neurosurgical diseases, with the possibility of continued improvements to image quality and enhanced access to neuroimaging in the future (Fig. 3). In the inpatient setting, delivery and acquisition of LF-MRI at the patient bedside enables continuity of medical care for patients with critical illness who depend on uninterrupted operation of specialized life support machinery[13,106]. LF-MRI is thus an invaluable tool in ICU settings that contain ferromagnetic material, including ventilators, monitors and infusion pumps. At the bedside, LF-MRI can serve as both a diagnostic device and a monitoring tool. The form factor allows for clinical staff to monitor the medical examination and life support parameters of a patient and administer medications throughout the time course of the LF-MRI examination itself[13,155,156]. Furthermore, patients who have contraindications for conventional MR (such as implantable pacemakers and metallic foreign metal bodies) could be good candidates for

portable LF-MRI in the future[14], although validation of this scenario awaits comprehensive evaluation (Box 2). The applications of LF-MRI can also extend beyond the hospital to pre-hospital environments, encompassing community health facilities, urgent care centres and mobile imaging. LF-MRI situated in community health centres can benefit patients who require interval imaging for neurological disease monitoring and therapeutic intervention titration, enabling more frequent scans of individuals at less cost and greater convenience. Point-of-care imaging in the clinic or at other locations (that is, infusion centre or patient home) could also improve surveillance of patients with systemic malignancy who require scans to monitor for central nervous system metastasis, providing earlier intervention for major adverse events. Community-level screening of patients at risk of neurological disease using LF-MRI could also enhance the identification, diagnosis and initiation of potentially modifiable treatment to improve brain health in the population. For this purpose, LF-MRI technology on mobile ambulances with telemedicine capabilities could be used, providing advantages for patients who have limited mobility and/or are bed-bound in their residential premises[157]. The feasibility of mobile MRI scanning has recently been demonstrated following deployment of a mobile, modified cargo van with an onboard LF-MRI scanner[150]. Nevertheless, scanning outside of conventional hospital environments will introduce ethical, legal and social issues that require careful consideration (Box 3).

In addition to community-based screening, ambulance-based LF-MRI scanning could improve the diagnosis of disease processes that have overlapping clinical features and optimize triage algorithms for patient transport to appropriate facilities through emergency medical services. For stroke, the advent of mobile ambulances equipped with portable CT scanners and specialized personnel onboard or accessible by telemedicine, have not only demonstrated benefits in the faster delivery of time-sensitive thrombolytic treatment to patients but have also shown superiority in reducing stroke disability as compared to standard pre-hospital emergency medical services[96,158,159]. Given the unique sensitivity of MRI to acute stroke, mobile LF-MRI ambulances could expand the delivery of expedited stroke care and facilitate the earlier identification of patients who might otherwise be excluded from treatment. The use of multimodal imaging in ambulances equipped with portable LF-MRI scanners could also inform patient selection procedures for stroke with unknown time of onset using FLAIR and DWI imaging, a limitation of current mobile CT scanners.

Despite potential, LF-MRI systems are currently limited in the spectrum of sequences that have been developed and implemented, which might impact their clinical application. This drawback holds for SWI, which would greatly improve intracranial haemorrhage detection, MR angiography for detecting large vessel occlusion[155], and MR perfusion for detecting ischaemic core versus penumbra. The role of LF-MRI in contrast-based imaging is also yet to be realized. Contrast enhancement on LF-MRI using gadolinium-based agents is limited given the need to substantially increase dosing[160,161]. Determination of the ideal contrast agent for use at LF is needed and could include superpara-magnetic iron oxide nanoparticles[162] or macrocyclic gadolinium-based agents[163]. Formal validation of LF-MRI across a range of environments, populations and clinical applications represents an avenue for future research to position LF-MRI for widespread use.

Portable LF-MRI has the potential to bring the advantages of MR technology to a wider population, circumventing some of the limitations associated with high magnetic field strength. In the immediate future, it is likely that portable LF-MRI will serve a distinct niche, given its lower resolution and limited sequences. With continued improvements in image acquisition and post-processing techniques, formal clinical validation studies will highlight use-case scenarios for diagnostic neuroimaging. Serial examinations will allow clinicians improved insight into the evolution of the clinical course of patients.

Taken together, portable LF-MRI has the potential to democratize MRI. The experience to date highlights a common axiom in MR technology: advances that seemed impossible years earlier have consistently become reality with time and research.

Acknowledgements

W.T.K., J.E.I., M.S.R. and K.N.S. are funded by a National Institute of Biomedical Imaging and Bioengineering R01 (EB031114-01A1). A.J.S.-A. is funded by the Fulbright Commission. A.G.W. is supported by an ERC Advanced Grant (101021218, PASMAR), an NWO-Open Technology grant (18981), and an NWO Stevin Prijs. E.X.W. is supported by Hong Kong Research Grant Council (R7003-19, HKU17112120, HKU17127121 and HKU17127022) and Lam Woo Foundation. F.X.S work is supported by NIH/NIMH grant RF1MH123698 on “Highly Portable and Cloud-Enabled Neuroimaging Research: Confronting Ethics in Field Research with New Populations.” The content is solely the responsibility of the authors and does not necessarily represent the official views of NIMH or NIH. S.J.S. is supported by NIH Director’s Transformative Award (1R01AI145057), and NIH grants (2R01HD085853-07, 1R01HD096693-01, 1U01NS107486 and 1UG3NS123307). J.E.I. is funded by Alzheimer’s Research UK (ARUK-IRG2019A-003), NIH BRAIN Initiative (1RF1MH123195, 1UM1MH130981) and NIH grant (1R01AG07098). M.S.R. acknowledges the gracious support of the Kiyomi and Ed Baird MGH Research Scholar Award. All other co-authors report no relevant disclosures or funding.

References

1. Pfahler GE In Proceedings of the 5th Annual Meeting of the American Roentgen Ray Society Vol. 4, 175–183 (St. Louis, MO, 1904).
2. Burr CW, Pfahler GE & Camp CD Thrombosis of the midcerebral artery, causing aphasia and hemiplegia, with remarks on cerebral skiagraphy. J. Nerv. Ment. Dis 31, 558 (1904).
3. Ambrose J Computerized transverse axial scanning (tomography). 2. Clinical application. Br. J. Radiol 46, 1023–1047 (1973). [PubMed: 4757353]
4. Hounsfield GN Computerized transverse axial scanning (tomography). 1. Description system. Br. J. Radiol 46, 1016–1022 (1973). [PubMed: 4757352]
5. Lauterbur PC Image formation by induced local interactions. Examples employing nuclear magnetic resonance. 1973.Clin. Orthop. Relat. Res 244, 3–6 (1989).
6. Mansfield P & Maudsley AA Planar spin imaging by NMR. J. Magn. Reson 27, 101–119 (1977).
7. Raich H & Blümler P Design and construction of a dipolar Halbach array with a homogeneous field from identical bar magnets: NMR Mandhalas. Concepts Magn. Reson. Part B Magn. Reson. Eng 23B, 16–25 (2004).
8. Lother S, Schiff SJ, Neuberger T, Jakob PM & Fidler F Design of a mobile, homogeneous, and efficient electromagnet with a large field of view for neonatal low-field MRI. Magn. Reson. Mater. Phys. Biol. Med 29, 691–698 (2016).
9. Obungoloch J et al. Design of a sustainable prepolarizing magnetic resonance imaging system for infant hydrocephalus. Magnetic Reson. Mater. Phys. Biol. Med 31, 665–676 (2018).
10. Harper JR et al. An unmatched radio frequency chain for low-field magnetic resonance imaging. Front. Phys 10.3389/fphy.2021.727536 (2022).
11. Sarracanie M et al. Low-cost high-performance MRI. Sci. Rep 5, 15177 (2015). [PubMed: 26469756]
12. He Y et al. Use of 2.1 MHz MRI scanner for brain imaging and its preliminary results in stroke. J. Magn. Reson 319, 106829 (2020). [PubMed: 32987217]

13. Sheth KN et al. Assessment of brain injury using portable, low-field magnetic resonance imaging at the bedside of critically ill patients. JAMA Neurol. 78, 41–47 (2020). [PubMed: 32897296]
14. Liu Y et al. A low-cost and shielding-free ultra-low-field brain MRI scanner. Nat. Commun 12, 7238 (2021). [PubMed: 34907181]
15. Halbach K Design of permanent multipole magnets with oriented rare earth cobalt material. Nucl. Instrum. Methods 169, 1–10 (1980).
16. Blümler P & Casanova F In Mobile NMR and MRI: Developments and Applications 133–157 (The Royal Society of Chemistry, 2016).
17. Soltner H & Blümler P Dipolar Halbach magnet stacks made from identically shaped permanent magnets for magnetic resonance. Concepts Magn. Reson. Part A 36, 211–222 (2010).
18. Cooley CZ et al. Two-dimensional imaging in a lightweight portable MRI scanner without gradient coils. Magn. Reson. Med 73, 872–883 (2015). [PubMed: 24668520]
19. Stockmann JP, Cooley CZ, Guerin B, Rosen MS & Wald LL Transmit array spatial encoding (TRASE) using broadband WURST pulses for RF spatial encoding in inhomogeneous B0 fields. J. Magn. Reson 268, 36–48 (2016). [PubMed: 27155906]
20. Cooley CZ et al. A portable scanner for magnetic resonance imaging of the brain. Nat. Biomed. Eng 5, 229–239 (2021). [PubMed: 33230306]
21. Cooley CZ et al. Design of sparse Halbach magnet arrays for portable MRI using a genetic algorithm. IEEE Trans. Magn 10.1109/tmag.2017.2751001 (2018).
22. Martens MA et al. Insertable biplanar gradient coils for magnetic resonance imaging. Rev. Sci. Instrum 62, 2639–2645 (1991).
23. While PT, Forbes LK & Crozier S 3D gradient coil design for open MRI systems. J. Magn. Reson 207, 124–133 (2010). [PubMed: 20850360]
24. Zhang R et al. An optimized target-field method for MRI transverse biplanar gradient coil design. Meas. Sci. Technol 22, 125505 (2011).
25. Matsuzawa K, Abe M, Kose K & Terada Y Oval gradient coils for an open magnetic resonance imaging system with a vertical magnetic field. J. Magn. Reson 278, 51–59 (2017). [PubMed: 28359940]
26. Shen S, Koonjoo N, Kong X, Rosen MS & Xu Z Gradient coil design and optimization for an ultra-low-field MRI system. Appl. Magn. Reson 53, 895–914 (2022).
27. de Vos B, Fuchs P, O'Reilly T, Webb A & Remis R Gradient coil design and realization for a halbach-based MRI system. IEEE Trans. Magn 56, 1–8 (2020).
28. Přibil J, Přibilová A & Frollo I Vibration and noise in magnetic resonance imaging of the vocal tract: differences between whole-body and open-air devices. Sensors 10.3390/s18041112 (2018).
29. Sharp JC & King SB MRI using radiofrequency magnetic field phase gradients. Magn. Reson. Med 63, 151–161 (2010). [PubMed: 19918899]
30. Wang P et al. Correcting image distortions from a nonlinear B +1-gradient field in frequency-modulated Rabi-encoded echoes. Magn. Reson. Med 10.1002/mrm.29549 (2022).
31. Torres E et al. B(1)-gradient-based MRI using frequency-modulated Rabi-encoded echoes. Magn. Reson. Med 87, 674–685 (2022). [PubMed: 34498768]
32. Gruber B, Froeling M, Leiner T & Klomp DWJ RF coils: a practical guide for nonphysicists. J. Magn. Reson. Imaging 48, 590–604 (2018). [PubMed: 29897651]
33. Shen S et al. An optimized quadrature RF receive coil for very-low-field (50.4 mT) magnetic resonance brain imaging. J. Magn. Reson 342, 107269 (2022). [PubMed: 35905530]
34. O'Reilly T, Teeuwisse WM, de Gans D, Koolstra K & Webb AG In vivo 3D brain and extremity MRI at 50 mT using a permanent magnet Halbach array. Magn. Reson. Med 85, 495–505 (2021). [PubMed: 32627235]
35. Shen S, Xu S, Koonjoo N & Rosen MS Optimization of a close-fitting volume RF coil for brain imaging at 6.5 mT using linear programming. IEEE Trans. Biomed. Eng 68, 1106–1114 (2021). [PubMed: 32746026]
36. de Vos B et al. Design, characterisation and performance of an improved portable and sustainable low-field MRI system. Front. Phys 10.3389/fphy.2021.701157 (2021).

37. Tewari S, Yousefi S & Webb A Deep neural-network based optimization for the design of a multi-element surface magnet for MRI applications. Inverse Probl. 10.1088/1361-6420/ac492a (2022).
38. Giovannetti G & Menichetti L Litz wire RF coils for low frequency NMR applications. Measurement 110, 116–120 (2017).
39. Miltner O et al. Portable NMR-MOUSE (R): a new method and its evaluation of the Achilles tendon. Z. Orthop. Grenzgeb 141, 148–152 (2003).
40. Perlo J, Casanova F & Blumich B 3D imaging with a single-sided sensor: an open tomograph. J. Magn. Reson 166, 228–235 (2004). [PubMed: 14729034]
41. Perlo J et al. Desktop MRI as a promising tool for mapping intra-aneurismal flow. Magn. Reson. Imaging 33, 328–335 (2015). [PubMed: 25527392]
42. Srinivas SA et al. External dynamic interference estimation and removal (EDITER) for low field MRI. Magn. Reson. Med 10.1002/mrm.28992 (2021).
43. Srinivas SA, Cooley CZ, Stockmann JP, McDaniel PC & Wald LL In Proceedings of International Society of Magnetic Resonance in Medicine 1269 (2020).
44. Rearick T, Charvat GL, Rosen MS & Rothberg JM Noise Supression Methods and Apparatus. United States of America Patent US9797971B2 (2017).
45. Yuen MM et al. Portable, low-field magnetic resonance imaging enables highly accessible and dynamic bedside evaluation of ischemic stroke. Sci. Adv 8, eabm3952 (2022). [PubMed: 35442729]
46. Dyvorne H et al. Freeing MRI from its Faraday cage with Interference Rejection. Proceedings of the International Society for Magnetic Resonance in Medicine 749 (2021).
47. Zhao Y, Xiao L, Liu Y, Leong ATL & Wu EX Electromagnetic interference elimination via active sensing and deep learning prediction for radiofrequency shielding-free MRI. NMR Biomed. 3864 (2023).
48. Kibret B, Teshome AK & Lai DTH Analysis of the human body as an antenna for wireless implant communication. IEEE Trans. Antennas Propag 64, 1466–1476 (2016).
49. Sen S, Maity S & Das D The body is the network: to safeguard sensitive data, turn flesh and tissue into a secure wireless channel. IEEE Spectr. 57, 44–49 (2020).
50. Ingle V, Kogon S & Manolakis D Statistical and Adaptive Signal Processing (Artech, 2005).
51. Stearns SD In Advanced Topics in Signal Processing 246–288 (Prentice-Hall, Inc., 1987).
52. Lu H et al. Routine clinical brain MRI sequences for use at 3.0 Tesla. J. Magn. Reson. Imaging 22, 13–22 (2005). [PubMed: 15971174]
53. O'Reilly T & Webb AG In vivo T1 and T2 relaxation time maps of brain tissue, skeletal muscle, and lipid measured in healthy volunteers at 50 mT. Magn. Reson. Med 10.1002/mrm.29009 (2021).
54. Ma D et al. Magnetic resonance fingerprinting. Nature 495, 187–192 (2013). [PubMed: 23486058]
55. Zhu B, Liu JZ, Cauley SF, Rosen BR & Rosen MS Image reconstruction by domain-transform manifold learning. Nature 555, 487–492 (2018). [PubMed: 29565357]
56. Lin DJ, Johnson PM, Knoll F & Lui YW Artificial intelligence for MR image reconstruction: an overview for clinicians. J. Magn. Reson. Imaging 53, 1015–1028 (2021). [PubMed: 32048372]
57. Xiao L et al. Partial Fourier reconstruction of complex MR images using complex-valued convolutional neural networks. Magn. Reson. Med 87, 999–1014 (2022). [PubMed: 34611904]
58. Koonjoo N, Zhu B, Cody Bagnall G, Bhutto D & Rosen MS Boosting the signal-to-noise of low-field MRI with deep learning image reconstruction. Sci. Rep 11, 8248 (2021). [PubMed: 33859218]
59. Waddington DEJ et al. Real-time radial reconstruction with domain transform manifold learning for MRI-guided radiotherapy. Med Phys. 50, 1962–1974 (2023). [PubMed: 36646444]
60. Lecun Y, Bottou L, Bengio Y & Haffner P Gradient-based learning applied to document recognition. Proc. IEEE 86, 2278–2324 (1998).
61. Wang Z, Chen J & Hoi SCH Deep learning for image super-resolution: a survey. IEEE Trans. Pattern Anal. Mach. Intell 43, 3365–3387 (2021). [PubMed: 32217470]

62. Yang W et al. Deep learning for single image super-resolution: a brief review. IEEE Trans. Multimed 21, 3106–3121 (2019).
63. Cherukuri V, Guo T, Schiff SJ & Monga V Deep MR brain image super-resolution using spatio-structural priors. IEEE Trans. Image Process 10.1109/tip.2019.2942510 (2019).
64. Goodfellow I et al. Generative adversarial networks. Adv. Neural Inf. Process. Syst 10.1145/3422622 (2014).
65. Song TA, Chowdhury SR, Yang F & Dutta J PET image super-resolution using generative adversarial networks. Neural Netw. 125, 83–91 (2020). [PubMed: 32078963]
66. Sotiras A, Davatzikos C & Paragios N Deformable medical image registration: a survey. IEEE Trans. Med. Imaging 32, 1153–1190 (2013). [PubMed: 23739795]
67. Kondrateva E et al. Domain Sshift in Computer Vision Models for MRI Data Analysis: An Overview. Vol. 11605 (SPIE, 2021).
68. Wang M & Deng W Deep visual domain adaptation: a survey. Neurocomputing 312, 135–153 (2018).
69. Iglesias J et al. Quantitative Brain Morphometry of Portable Low-Field-Strength MRI Using Super-Resolution Machine Learning. Radiology 306, 3 (2023).
70. Tobin J et al. Domain randomization for transferring deep neural networks from simulation to the real world. IEEE/RSJ International Conference on Intelligent Robots and Systems (IROS), 23–30 (IEEE, 2017).
71. Cohen J, Luck M & Honari S In Medical Image Computing and Computer Assisted Intervention – MICCAI 2018 (eds Frangi A et al.), 529–536, (Springer, 2018).
72. Malinin A & Gales M In Proceedings of the 32nd International Conference on Neural Information Processing Systems 7047–7058 (Curran Associates Inc., 2018).
73. Kendall A & Gal Y What uncertainties do we need in Bayesian deep learning for computer vision? 31st Conference on Neural Information Processing Systems vol. 30 (NIPS, 2017).
74. Gal Y & Ghahramani Z Dropout as a Bayesian approximation: representing model uncertainty in deep learning. PMLR 48, 1050–1059 (2016).
75. Lakshminarayanan B, Pritzel A & Blundell C Simple and scalable predictive uncertainty estimation using deep ensembles. 31st Conference on Neural Information Processing Systems 6405–6416 (2017).
76. Sensoy M, Kaplan L & Kandemir M In Proceedings of the 32nd International Conference on Neural Information Processing Systems 3183–3193 (Curran Associates Inc., 2018).
77. Mehrabi N, Morstatter F, Saxena N, Lerman K & Galstyan A A survey on bias and fairness in machine learning. ACM Comput. Surv 54, 1–35 (2021).
78. Petersen E et al. Feature robustness and sex differences in medical imaging: a case study in MRI-based Alzheimer's disease detection. In Medical Image Computing and Computer Assisted Intervention – MICCAI 2022: 25th International Conference Proceedings 88–98 (2022).
79. Dressel J & Farid H The accuracy, fairness, and limits of predicting recidivism. Sci. Adv 4, eaao5580 (2018). [PubMed: 29376122]
80. Larson J, Mattu S, Kirchner L & Angwin J Machine Bias https://www.propublica.org/article/machine-bias-risk-assessments-in-criminal-sentencing ProPublica (2016).
81. Chouldechova A, Benavides-Prado D, Fialko O & Vaithianathan R In Proceedings of the 1st Conference on Fairness, Accountability and Transparency Vol. 81 (eds Sorelle AF & Christo W) 134–148 (Proceedings of Machine Learning Research, 2018).
82. Puyol Anton E et al. Fairness in AI: are deep learning-based CMR segmentation algorithms biased. Eur. Heart J 10.1093/eurheartj/ehab724.3055 (2021).
83. Ruijsink B et al. Fully automated, quality-controlled cardiac analysis from CMR: validation and large-scale application to characterize cardiac function. JACC: Cardiovasc. Imaging 13, 684–695 (2019). [PubMed: 31326477]
84. Bellamy RKE et al. AI Fairness 360: An extensible toolkit for detecting and mitigating algorithmic bias. IBM J. Res. Dev 10.1147/JRD.2019.2942287 (2019).

85. Chalela JA et al. Magnetic resonance imaging and computed tomography in emergency assessment of patients with suspected acute stroke: a prospective comparison. Lancet 369, 293–298 (2007). [PubMed: 17258669]
86. Campbell BC & Parsons MW Imaging selection for acute stroke intervention. Int. J. Stroke 13, 554–567 (2018). [PubMed: 29543140]
87. Shah S et al. Screening with MRI for accurate and rapid stroke treatment: SMART. Neurology 84, 2438–2444 (2015). [PubMed: 25972494]
88. Sorensen AG et al. Hyperacute stroke: evaluation with combined multisection diffusion-weighted and hemodynamically weighted echo-planar MR imaging. Radiology 199, 391–401 (1996). [PubMed: 8668784]
89. Fiebach JB et al. CT and diffusion-weighted MR imaging in randomized order: diffusion-weighted imaging results in higher accuracy and lower interrater variability in the diagnosis of hyperacute ischemic stroke. Stroke 33, 2206–2210 (2002). [PubMed: 12215588]
90. Thomalla G et al. Intravenous alteplase for stroke with unknown time of onset guided by advanced imaging: systematic review and meta-analysis of individual patient data. Lancet 396, 1574–1584 (2020). [PubMed: 33176180]
91. Powers WJ et al. Guidelines for the early management of patients with acute ischemic stroke: 2019 update to the 2018 guidelines for the early management of acute ischemic stroke: a guideline for healthcare professionals from the American Heart Association/American Stroke Association. Stroke 50, e344–e418 (2019). [PubMed: 31662037]
92. Thomalla G et al. DWI-FLAIR mismatch for the identification of patients with acute ischaemic stroke within 4.5 h of symptom onset (PRE-FLAIR): a multicentre observational study. Lancet Neurol. 10, 978–986 (2011). [PubMed: 21978972]
93. Kidwell CS et al. Comparison of MRI and CT for detection of acute intracerebral hemorrhage. J. Am. Med. Assoc 292, 1823–1830 (2004).
94. Yuen MM et al. Qualitative description of ischemic stroke appearance on low-field, point-of-care magnetic resonance imaging. Stroke 52, A33–A33 (2021).
95. Mazurek MH et al. Portable, bedside, low-field magnetic resonance imaging for evaluation of intracerebral hemorrhage. Nat. Commun 12, 5119 (2021). [PubMed: 34433813]
96. Grotta JC et al. Prospective, multicenter, controlled trial of mobile stroke units. N. Engl. J. Med 385, 971–981 (2021). [PubMed: 34496173]
97. Lahner D et al. Incidence of complications in intrahospital transport of critically ill patients–experience in an Austrian university hospital. Wien. Klin. Wochenschr 119, 412–416 (2007). [PubMed: 17671822]
98. Papson JP, Russell KL & Taylor DM Unexpected events during the intrahospital transport of critically ill patients. Acad. Emerg. Med 14, 574–577 (2007). [PubMed: 17535981]
99. Venkategowda PM, Rao SM, Mutkule DP & Taggu AN Unexpected events occurring during the intra-hospital transport of critically ill ICU patients. Indian J. Crit. Care Med 18, 354–357 (2014). [PubMed: 24987233]
100. Knight PH et al. Complications during intrahospital transport of critically ill patients: focus on risk identification and prevention. Int. J. Crit. Illn. Inj. Sci 5, 256–264 (2015). [PubMed: 26807395]
101. Andrews PJ, Piper IR, Dearden NM & Miller JD Secondary insults during intrahospital transport of head-injured patients. Lancet 335, 327–330 (1990). [PubMed: 1967776]
102. Kaups KL, Davis JW & Parks SN Routinely repeated computed tomography after blunt head trauma: does it benefit patients? J. Trauma Acute Care Surg 56, 475–480 (2004).
103. Martin M et al. Secondary insults and adverse events during intrahospital transport of severe traumatic brain-injured patients. Neurocrit. Care 26, 87–95 (2017). [PubMed: 27601068]
104. Smith I, Fleming S & Cernaianu A Mishaps during transport from the intensive care unit. Crit. Care Med 18, 278–281 (1990). [PubMed: 2302952]
105. Beekman R et al. Bedside monitoring of hypoxic ischemic brain injury using low-field, portable brain magnetic resonance imaging after cardiac arrest. Resuscitation 176, 150–158 (2022). [PubMed: 35562094]

106. Cho SM et al. Assessing the safety and feasibility of bedside portable low-field brain magnetic resonance imaging in patients on ECMO (SAFE-MRI ECMO study): study protocol and first case series experience. Crit. Care 26, 119 (2022). [PubMed: 35501837]
107. Turpin J et al. Portable magnetic resonance imaging for ICU patients. Crit. Care Explor 2, e0306 (2020). [PubMed: 33381764]
108. Lopez Soto C et al. Imaging for neuroprognostication after cardiac arrest: systematic review and meta-analysis. Neurocrit. Care 32, 206–216 (2020). [PubMed: 31549351]
109. Maciel CB, Barden MM, Youn TS, Dhakar MB & Greer DM Neuroprognostication practices in postcardiac arrest patients: an international survey of critical care providers. Crit. Care Med 48, e107–e114 (2020). [PubMed: 31939809]
110. Peterson MR et al. Normal childhood brain growth and a universal sex and anthropomorphic relationship to cerebrospinal fluid. J. Neurosurg. Pediatr 28, 458–468 (2021). [PubMed: 34243147]
111. Bethlehem RAI et al. Brain charts for the human lifespan. Nature 604, 525–533 (2022). [PubMed: 35388223]
112. Cherukuri V et al. Learning based segmentation of CT brain images: application to postoperative hydrocephalic scans. Transl. Biomed. Eng 65, 1871–1884 (2018).
113. Deoni SCL et al. Accessible pediatric neuroimaging using a low field strength MRI scanner. NeuroImage 238, 118273 (2021). [PubMed: 34146712]
114. Whitby EH et al. Ultrafast magnetic resonance imaging of the neonate in a magnetic resonance-compatible incubator with a built-in coil. Pediatrics 113, e150–e152 (2004). [PubMed: 14754986]
115. Bekiesinska-Figatowska M et al. First experience with neonatal examinations with the use of MR-compatible incubator. Pol. J. Radiol 79, 268–274 (2014). [PubMed: 25152798]
116. Sien ME et al. Feasibility of and experience using a portable MRI scanner in the neonatal intensive care unit. Arch. Dis. Childhood. Fetal Neonatal Ed 108, 45–50 (2023). [PubMed: 35788031]
117. Mathur AM, Neil JJ, McKinstry RC & Inder TE Transport, monitoring, and successful brain MR imaging in unsedated neonates. Pediatr. Radiol 38, 260–264 (2008). [PubMed: 18175110]
118. Whitby EH et al. Low field strength magnetic resonance imaging of the neonatal brain. Arch. Dis. Child. Fetal Neonatal Ed 88, F203–F208 (2003). [PubMed: 12719393]
119. Karimy JK et al. Inflammation in acquired hydrocephalus: pathogenic mechanisms and therapeutic targets. Nat. Rev. Neurol 16, 285–296 (2020). [PubMed: 32152460]
120. Sinnar SA & Schiff SJ The problem of microbial dark matter in neonatal sepsis. Emerg. Infect. Dis 26, 2543–2548 (2020). [PubMed: 33080169]
121. Paulson JN et al. Paenibacillus infection with frequent viral coinfection contributes to postinfectious hydrocephalus in Ugandan infants. Sci. Transl. Med 10.1126/scitranslmed.aba0565 (2020).
122. Kulkarni AV et al. Endoscopic treatment versus shunting for infant hydrocephalus in Uganda. N. Engl. J. Med 377, 2456–2464 (2017). [PubMed: 29262276]
123. Schiff SJ et al. Brain growth after surgical treatment for infant postinfectious hydrocephalus in sub-Saharan Africa: 2-year results of a randomized trial. J. Neurosurg. Pediatr 10.3171/2021.2.PEDS20949 (2021).
124. Brenner DJ & Hall EJ Computed tomography — an increasing source of radiation exposure. N. Engl. J. Med 357, 2277–2284 (2007). [PubMed: 18046031]
125. Lane JR et al. Preoperative risk and postoperative outcome from subdural fluid collections in African infants with postinfectious hydrocephalus. J. Neurosurg. Pediatr 29, 31–39 (2022). [PubMed: 34598146]
126. Harper JR et al. Assessing the utility of low resolution brain imaging: treatment of infant hydrocephalus. Neuroimage Clin. 32, 102896 (2021). [PubMed: 34911199]
127. Bos D et al. Prevalence, clinical management, and natural course of incidental findings on brain MR images: the population-based Rotterdam Scan Study. Radiology 281, 507–515 (2016). [PubMed: 27337027]

128. Bunnik EM & Vernooij MW Incidental findings in population imaging revisited. Eur. J. Epidemiol 31, 1–4 (2016).
129. Gibson LM et al. Potentially serious incidental findings on brain and body magnetic resonance imaging of apparently asymptomatic adults: systematic review and meta-analysis. BMJ 363, k4577 (2018). [PubMed: 30467245]
130. Ivanovic V et al. Prevalence of incidental brain MRI findings of clinical relevance in a diverse Hispanic/Latino population. J. Neuroimaging 31, 1166–1175 (2021). [PubMed: 34288226]
131. Vernooij MW et al. Incidental findings on brain MRI in the general population. N. Engl. J. Med 357, 1821–1828 (2007). [PubMed: 17978290]
132. Neugut AI et al. Magnetic resonance imaging-based screening for asymptomatic brain tumors: a review. Oncologist 24, 375–384 (2019). [PubMed: 30305414]
133. Gupta S et al. Challenges and possible solutions to colorectal cancer screening for the underserved. J. Natl Cancer Inst 106, dju032 (2014).
134. Neal CD et al. Patient navigation to improve cancer screening in underserved populations: reported experiences, opportunities, and challenges. J. Am. Coll. Radiol 15, 1565–1572 (2018). [PubMed: 29685346]
135. Bryan RN et al. Prevalence and anatomic characteristics of infarct-like lesions on MR images of middle-aged adults: the atherosclerosis risk in communities study. Am. J. Neuroradiol 20, 1273–1280 (1999). [PubMed: 10472985]
136. Liao D et al. Presence and severity of cerebral white matter lesions and hypertension, its treatment, and its control. The ARIC Study. Atherosclerosis risk in communities study. Stroke 27, 2262–2270 (1996). [PubMed: 8969791]
137. Prabhakaran S et al. Prevalence and determinants of subclinical brain infarction: the Northern Manhattan study. Neurology 70, 425–430 (2008). [PubMed: 17898325]
138. Poels MMF et al. Incidence of cerebral microbleeds in the general population. Stroke 42, 656–661 (2011). [PubMed: 21307170]
139. Au R et al. Association of white matter hyperintensity volume with decreased cognitive functioning: the Framingham heart study. Arch. Neurol 63, 246–250 (2006). [PubMed: 16476813]
140. Debette S & Markus HS The clinical importance of white matter hyperintensities on brain magnetic resonance imaging: systematic review and meta-analysis. BMJ 341, c3666 (2010). [PubMed: 20660506]
141. Debette S, Schilling S, Duperron MG, Larsson SC & Markus HS Clinical significance of magnetic resonance imaging markers of vascular brain injury: a systematic review and meta-analysis. JAMA Neurol. 76, 81–94 (2019). [PubMed: 30422209]
142. de Havenon A et al. Blood pressure, glycemic control, and white matter hyperintensity progression in type 2 diabetics. Neurology 92, e1168–e1175 (2019). [PubMed: 30737332]
143. Nasrallah IM et al. Association of intensive vs standard blood pressure control with cerebral white matter lesions. J. Am. Med. Assoc 322, 524–534 (2019).
144. Sheibani N et al. White matter hyperintensity and cardiovascular disease outcomes in the SPRINT MIND trial. J. Stroke Cerebrovasc. Dis 30, 105764 (2021). [PubMed: 33823461]
145. Williamson JD et al. Effect of intensive vs standard blood pressure control on probable dementia: a randomized clinical trial. J. Am. Med. Assoc 321, 553–561 (2019).
146. de Havenon A et al. Identification of white matter hyperintensities in routine emergency department visits using portable bedside magnetic resonance imaging. J. Am. Heart Assoc 12, e029242 (2023). [PubMed: 37218590]
147. Ross AB et al. Racial and/or ethnic disparities in the use of imaging: results from the 2015 National Health Interview Survey. Radiology 302, 140–142 (2022). [PubMed: 34726530]
148. Arnold TC et al. Portable, low-field magnetic resonance imaging sensitively detects and accurately quantifies multiple sclerosis lesions. NeuroImage: Clinical 35, 103101 (2022). [PubMed: 35792417]
149. Arnold TC et al. Sensitivity of portable low-field magnetic resonance imaging for multiple sclerosis lesions. NeuroImage Clin. 35, 103101 (2022). [PubMed: 35792417]

150. Deoni SCL et al. Development of a mobile low-field MRI scanner. Sci. Rep 12, 5690 (2022). [PubMed: 35383255]
151. Schrager JD et al. Racial and ethnic differences in diagnostic imaging utilization during adult emergency department visits in the United States, 2005 to 2014. J. Am. Coll. Radiol 16, 1036–1045 (2019). [PubMed: 31092354]
152. Marin JR et al. Racial and ethnic differences in emergency department diagnostic imaging at US children's hospitals, 2016–2019. JAMA Netw. Open 4, e2033710 (2021). [PubMed: 33512517]
153. Haas JS et al. Disparities in the use of screening magnetic resonance imaging of the breast in community practice by race, ethnicity, and socioeconomic status. Cancer 122, 611–617 (2016). [PubMed: 26709819]
154. Ross AB, Kalia V, Chan BY & Li G The influence of patient race on the use of diagnostic imaging in United States emergency departments: data from the National Hospital Ambulatory Medical Care survey. BMC Health Serv. Res 20, 840 (2020). [PubMed: 32894129]
155. Sheth KN et al. Bedside detection of intracranial midline shift using portable magnetic resonance imaging. Sci. Rep 12, 67 (2022). [PubMed: 34996970]
156. Alexandrov AW et al. Perfusion augmentation in acute stroke using mechanical counter-pulsation-phase IIa: effect of external counterpulsation on middle cerebral artery mean flow velocity in five healthy subjects. Stroke 39, 2760–2764 (2008). [PubMed: 18658038]
157. Zubair AS, Crawford A, Prabhat AM & Sheth KN Use of portable imaging modalities in patients with neurologic disorders: a case-based discussion. Cureus 13, e15841 (2021). [PubMed: 34327077]
158. Parker SA et al. Establishing the first mobile stroke unit in the United States. Stroke 46, 1384–1391 (2015). [PubMed: 25782464]
159. Bowry R et al. Benefits of stroke treatment using a mobile stroke unit compared with standard management: the BEST-MSU study run-in phase. Stroke 46, 3370–3374 (2015). [PubMed: 26508753]
160. Brekenfeld C et al. Enhancement of cerebral diseases: how much contrast agent is enough? Comparison of 0.1, 0.2, and 0.3 mmol/kg gadoteridol at 0.2 T with 0.1 mmol/kg gadoteridol at 1.5 T. Investig. Radiol 36, 266–275 (2001). [PubMed: 11323514]
161. Desai NK & Runge VM Contrast use at low field: a review. Top. Magn. Reson. Imaging 14, 360–364 (2003). [PubMed: 14625464]
162. Waddington DEJ, Boele T, Maschmeyer R, Kuncic Z & Rosen MS High-sensitivity in vivo contrast for ultra-low field magnetic resonance imaging using superparamagnetic iron oxide nanoparticles. Sci. Adv 6, eabb0998 (2020). [PubMed: 32733998]
163. Van Zandwijk JK et al. Comparing the signal enhancement of a gadolinium based and an iron-oxide based contrast agent in low-field MRI. PLoS One 16, e0256252 (2021). [PubMed: 34403442]
164. Masouridis M, Dyrby TB & Zhurbenko V Design and implementation of solenoid and Alderman-Grant coils for magnetic resonance microscopy at 7T. in 2020 14th European Conference on Antennas and Propagation (EuCAP) 1–4 (2020).
165. Oh S, Hong SE & Choi HD Proposed safety guidelines for patient assistants in an open MRI Environment. Int. J. Environ. Res. Public Health 19, 15185 (2022). [PubMed: 36429902]
166. Marques JP, Simonis FFJ & Webb AG Low-field MRI: an MR physics perspective. J. Magn. Reson. Imaging 49, 1528–1542 (2019). [PubMed: 30637943]
167. Cooley CZ et al. Design of sparse Halbach magnet arrays for portable MRI using a genetic algorithm. IEEE Trans Magn. 54, 5100112 (2018). [PubMed: 29749974]
168. Huang S et al. Portable low-cost MRI system based on permanent magnets/magnet arrays. Investig. Magn. Reson. Imaging 23, 179–201 (2019).
169. Smith FW, Mallard JR, Reid A & Hutchison JM Nuclear magnetic resonance tomographic imaging in liver disease. Lancet 1, 963–966 (1981). [PubMed: 6112385]
170. Crooks L et al. Nuclear magnetic resonance whole-body imager operating at 3.5 KGauss. Radiology 143, 169–174 (1982). [PubMed: 7063722]
171. Bottomley PA et al. NMR imaging/spectroscopy system to study both anatomy and metabolism. Lancet 2, 273–274 (1983).

172. Hart HR Jr. et al. Nuclear magnetic resonance imaging: contrast-to-noise ratio as a function of strength of magnetic field. Am. J. Roentgenol 141, 1195–1201 (1983). [PubMed: 6606316]
173. Halbach K Application of permanent magnets in accelerators and electron storage rings (invited).J. Appl. Phys 57, 3605–3608 (1985).
174. Sepponen RE, Sipponen JT & Sivula A Low field (0.02 T) nuclear magnetic resonance imaging of the brain. J. Comput. Assist. Tomogr 9, 237–241 (1985). [PubMed: 3973144]
175. Bilaniuk LT et al. Cerebral magnetic resonance: comparison of high and low field strength imaging. Radiology 153, 409–414 (1984). [PubMed: 6541355]
176. Hittmair K, Kramer J, Rand T, Bernert G & Wimberger D Infratentorial brain maturation: a comparison of MRI at 0.5 and 1.5T. Neuroradiology 38, 360–366 (1996). [PubMed: 8738096]
177. Macovski A & Conolly S Novel approaches to low-cost MRI. Magn. Reson. Med 30, 221–230 (1993). [PubMed: 8366803]
178. Lee SK et al. SQUID-detected MRI at 132 microT with T1-weighted contrast established at 10 microT–300 mT. Magn. Reson. Med 53, 9–14 (2005). [PubMed: 15690496]
179. Tsai LL et al. Posture-dependent human ^{3}He lung imaging in an open-access MRI system: initial results. Acad. Radiol 15, 728–739 (2008). [PubMed: 18486009]
180. Zotev VS et al. Parallel MRI at microtesla fields. J. Magn. Reson 192, 197–208 (2008). [PubMed: 18328753]
181. Zotev VS et al. Microtesla MRI with dynamic nuclear polarization. J. Magn. Reson 207, 78–88 (2010). [PubMed: 20843715]
182. Sarracanie M, Armstrong BD, Stockmann J & Rosen MS High speed 3D overhauser-enhanced MRI using combined b-SSFP and compressed sensing. Magn. Reson. Med 71, 735–745 (2014). [PubMed: 23475813]
183. Schellhammer SM et al. Integrating a low-field open MR scanner with a static proton research beam line: proof of concept. Phys. Med. Biol 63, 23LT01 (2018).
184. Chetcuti K et al. Implementation of a low-field portable MRI scanner in a resource-constrained environment: our experience in Malawi. Am. J. Neuroradiol 43, 670–674 (2022). [PubMed: 35450856]
185. Prabhat AM et al. Methodology for low-field, portable magnetic resonance neuroimaging at the bedside. Front. Neurol 12, 760321 (2021). [PubMed: 34956049]
186. Bhat SS et al. Low-field MRI of stroke: challenges and opportunities. J. Magn. Reson. Imaging 54, 372–390 (2021). [PubMed: 32827173]
187. OECD. OECD Regions and Cities at a Glance 2020 https://www.oecd-ilibrary.org/urban-rural-and-regional-development/oecd-regions-and-cities-at-a-glance-2020_959d5ba0-en#:~:text=PDF%20%2D%20365.88KB-,Regions%20and%20Cities%20at%20a%20Glance%202020%20provides%20a%20comprehensive,more%20resilient%20economies%20and%20societies (2020).
188. Bierman H The safety of MRI. JAMA 261, 3412 (1989).
189. Russo RJ et al. Assessing the risks associated with MRI in patients with a pacemaker or defibrillator. N. Engl. J. Med 376, 755–764 (2017). [PubMed: 28225684]
190. Nazarian S et al. Safety of magnetic resonance imaging in patients with cardiac devices. N. Engl. J. Med 377, 2555–2564 (2017). [PubMed: 29281579]
191. Shen FX, Wolf SM, Gonzalez RG & Garwood M Ethical issues posed by field research using highly portable and cloud-enabled neuroimaging. Neuron 105, 771–775 (2020). [PubMed: 32135089]
192. Shen FX et al. Emerging ethical issues raised by highly portable MRI research in remote and resource-limited international settings. Neuroimage 238, 118210 (2021). [PubMed: 34062266]
193. Shen FX Highly Portable and Cloud-Enabled Neuroimaging Research: Confronting Ethics Challenges in Field Research with New Populations https://www.neuroimagingethics.org/ (2022).

Box 1

Low-resource considerations

Despite the widespread availability of MRI in certain countries, two-thirds of the global population lacks access to such technology[185,186]. In resource-constrained environments, the relative affordability and accessibility of low-field MRI (LF-MRI) technology compared with conventional MRI and CT provides an alternative to neuroimaging that would otherwise not be possible. This is true of low-income and middle-income countries as well as high-income countries whose populations are geographically dispersed[187]. In a low-income setting, LF-MRI has recently been deployed in sub-Saharan Africa[184]. This experience has identified several enablers and barriers to deploying LF-MRI in resource-constrained environments, as follows:

- Equipment storage: the lack of requirement for supercooling cryogens can facilitate deployment of LF-MRI in environments where access to liquid nitrogen and liquid helium might be limited. Storage environments equipped with temperature and humidity control are still necessary as optimal imaging on permanent magnet systems is temperature dependent.
- Logistics of operation: LF-MRI scanners are relatively simple to operate. Bioengineering solutions that facilitate motorized portability and operation through a streamlined tablet interface has simplified use. Furthermore, cloud-based imaging solutions have been implemented with the ability for users to upload images directly to picture-archiving and communication systems for expedited interpretation. Moreover, the lower magnetic field strength could eliminate some of the safety considerations that are present for high-field systems. However, until the safety and compatibility are well established at LF-MRI field strengths, MRI safety training is likely necessary.
- Adaptation to different patient populations: LF-MRI located in low-resource environments may enable clinicians to answer discreet questions relevant to the population such as cerebral malaria and cysticercosis, which are more prevalent in sub-Saharan Africa than in industrialized countries.
- Geographically dispersed populations: enhanced access to LF-MRI in countries whose populations are geographically dispersed may facilitate a decrease in long-standing health disparities in diagnosis of neurological disease owing to improved access to MR technologies.
- Research in low-resource settings: local communities could be made partners in the research enterprise, and the local social value of the research should be prioritized.
- Infrastructure stability: a stable electrical supply and adequate internet speed are both necessary to operate the scanner and upload images for interpretation. Poor IT infrastructure may impede access to technology and data-sharing capacities, in addition to the feasibility of performing regular software updates.

- Remote support: local engineering expertise for troubleshooting, hardware maintenance and repair is essential in low-resource settings, with lack of physical support limiting the ability to overcome instances of device malfunction. Despite provision of technical support online, this requires a stable internet connection. Depending on local regulations around the storage of health information, sufficient infrastructure to support image storage may be needed.

Box 2

Safety considerations

Safety considerations for conventional high-field MRI include thermal effects, acoustic noise and contraindications caused by ferromagnetic implants[188]. By way of thermal effects, MR exposure should avoid producing a core temperature increase greater than 1 °C (ref.188). Contraindications caused by metal implants encompass MR-incompatible aneurysm clips and those that are electrically, magnetically or mechanically activated such as pacemakers, defibrillators and neurostimulators. Although studies have reported an absence of substantial adverse events of scanning patients with in situ pacemakers or defibrillators[189,190], guidelines still preclude patients from routine imaging. Safety considerations on low-field MRI (LF-MRI) thus include consideration of the following:

- Projectile risk: no known risk.
- Thermal effects: thermal power deposition at LF is 1–2 orders of magnitude less than high-field MRI.
- Acoustic noise: the typical acoustic noises created by Lorentz forces during LF-MRI acquisition are below 70 decibels. Noise levels <70 decibels are unlikely to cause hearing loss even in the setting of prolonged exposure.
- Electronic implants: contraindications arising from implantable ferromagnetic materials (such as pacemakers and other foreign metal bodies) can theoretically be circumvented through use of LF-MRI. However, a comprehensive evaluation has not been conducted.
- Portability: the transport of a LF-MRI might lead to magnetic field exposures in new areas and environments.

Box 3

Translational considerations

The ability of low-field MRI (LF-MRI) to scan outside the conventional scanning environment will introduce a host of ethical, legal and social issues. Although LF-MRI scanners are portable, the expertise and additional facilities of a major hospital system cannot be easily transported. Thus, the research and clinical teams must ensure several factors: first, that safety and privacy protocols have been developed for each site where the LF-MRI scanner will be used; second, that the remote site has access to requisite expertise to direct the process of obtaining informed consent; third, that there is a plan in place to respond if follow-up care or a higher-resolution scan is warranted and cannot be provided at the remote site; and fourth, that there is compliance with laws and regulations in each of the jurisdictions where the scanner will be used and data will be shared[191]. A prerequisite to identifying and addressing these ethical, legal and social issue challenges is to encourage sustained engagement with the local communities and hospitals in which LF-MRI scanners will be deployed[192]. Prominent considerations[193] include the following:

- Access, inclusion and community engagement: to improve access, deployment of LF-MRI should include partnership and engagement with under-represented and under-resourced communities.
- Ensuring privacy: heightened privacy concerns may need to be addressed compared to fixed MRI, where only the patient and technician are in the scanning room; LF-MRI can be set up with minimal barriers surrounding the scanner and thus the scanning environment is significantly less secluded.
- Overlapping regulatory jurisdictions: a portable LF-MRI scanner that scans individuals in multiple states or countries will require the clinical or research teams to navigate multiple legal and regulatory environments to ensure successful data sharing and compliance with health and safety laws.
- Bias in artificial intelligence: if LF-MRI is being used in racially, ethnically and culturally diverse populations, results and images derived using artificial intelligence or machine learning models need to account for potential bias if the models have been trained on less diverse training data.
- Safeguards to avoid misuse: LF-MRI will allow for brain imaging to be used in new, commercially viable environments outside medicine, such as wellness spas and neurofeedback clinics, raising the potential for non-experts to either deliberately or inadvertently misinterpret or miscommunicate LF-MRI scan data. Safeguards should be put in place now to anticipate and mitigate these risks.

Key points

- Portable, low-field MRI (LF-MRI) has enabled scanning outside the controlled environment of a conventional MRI suite, enhancing access to neuroimaging for indications that are not well suited to existing technologies.
- Advancements in electromagnetic noise cancellation and machine learning reconstruction algorithms as well as new approaches to image enhancement seek to maximize the information extracted from the reduced signal-to-noise ratio of LF-MRI.
- The reduced fringe field and the transportability of LF-MR have expanded the imaging capacity for neurological conditions such as stroke, intracerebral haemorrhage, cardiac arrest, hydrocephalus and multiple sclerosis.
- Hardware developments, improvements in pulse sequences and image reconstruction, and validation of clinical utility across a range of environments will continue to accelerate LF-MRI into the future.

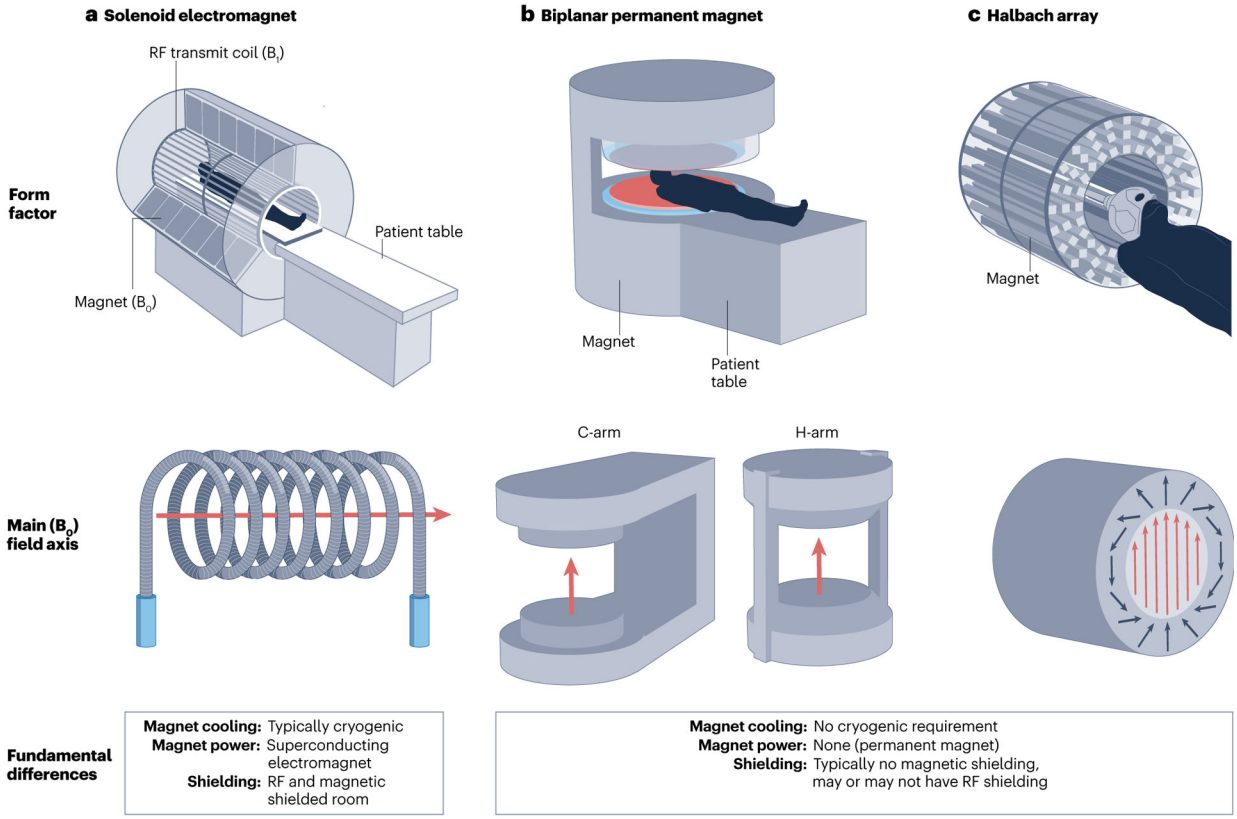

Fig. 1 |. Types of MRI geometries for portable LF-MRI.

a, Conventional solenoid MRI. **b**, Biplanar permanent low-field MRI (LF-MRI), including C-arm and H-arm geometries. **c**, Halbach array LF-MRI configuration. B_0, main magnetic field; B_1, radiofrequency field; RF, radiofrequency. Part **a**, upper panel, image courtesy of National High Magnetic Field Laboratory. Part **a**, bottom panel, adapted with permission from ref.164, IEEE. Part **b**, upper panel, adapted from ref.165, CC BY 4.0 (https://creativecommons.org/licenses/by/4.0/). Part **b**, bottom panel, adapted with permission from ref.166, Wiley. Part **c** upper panel © [2018] IEEE. Reprinted, with permission, from Cooley, C. Z., Haskell, M. W., Cauley, S. F., Sappo, C., Lapierre, C. D., Ha, C. G., Stockmann, J. P. & Wald, L. L. Design of sparse Halbach magnet arrays for portable MRI using a genetic algorithm. *IEEE Trans. Magn.* **54**, 5100112 (2018)[167]. Adaptation permission from author. Part **c**, bottom panel, adapted with permission from ref.168, iMRI.

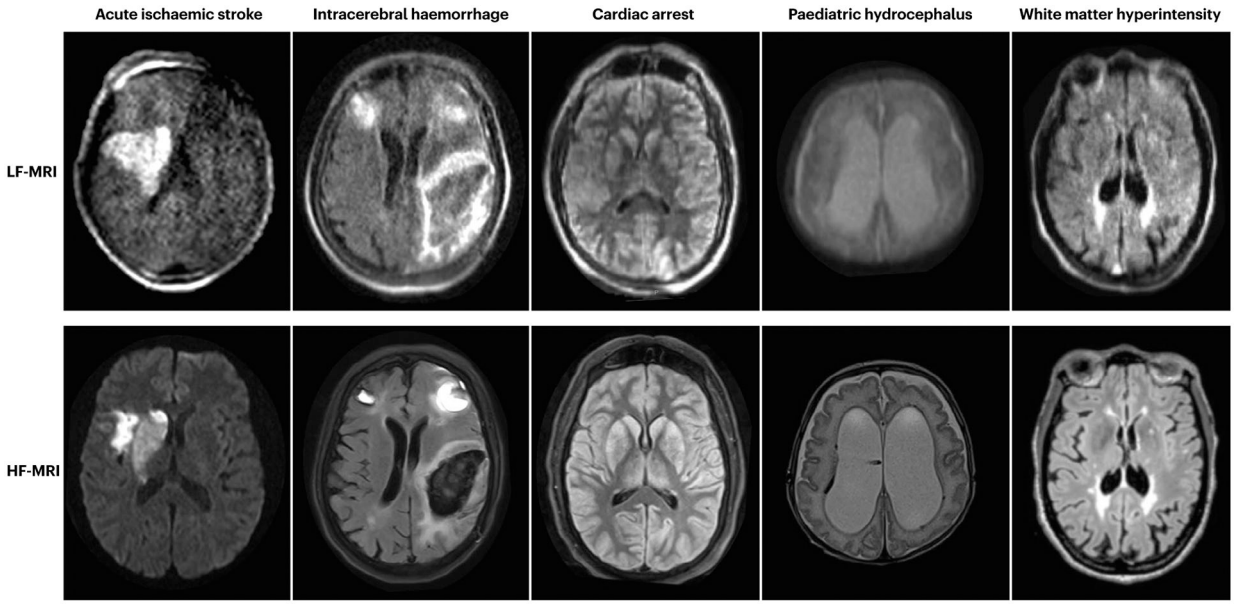

Fig. 2 |. Examples of images acquired on LF-MRI compared with conventional HF-MRI.
Clinical applications for low-field MRI (LF-MRI) include acute ischaemic stroke (diffusion-weighted imaging), intracerebral haemorrhage (T2 fluid-attenuated inversion recovery), cardiac arrest (T1-weighted imaging), paediatric hydrocephalus (T2-weighted imaging), and white matter hyperintensity (fluid- attenuated inversion recovery). Note the previously undetected region of ischaemia on LF-MRI diffusion-weighted imaging that was not detected on high-field MRI (HF-MRI) performed 3 days prior. All images were acquired on a 0.064 T portable LF-MRI (Hyperfine Research Inc.). HF-MRI and LF-MRI images of acute ischaemic stroke were adapted/reprinted from Science Advances ref.45. ©The Authors, some rights reserved; exclusive licensee AAAS. HF-MRI and LFMRI images of intracerebral haemorrhage reprinted from ref.95, Springer Nature Limited. HF-MRI and LF-MRI images of cardiac arrest reprinted with permission from ref.105, Elsevier. HF-MRI and LF-MRI images of paediatric hydrocephalus reproduced from ref.116 with permission from BMJ Publishing Group Ltd. HF-MRI and LF-MRI images of white matter hyperintensity were reprinted from ref.149, CC BY 4.0 (https://creativecommons.org/licenses/by/4.0/).

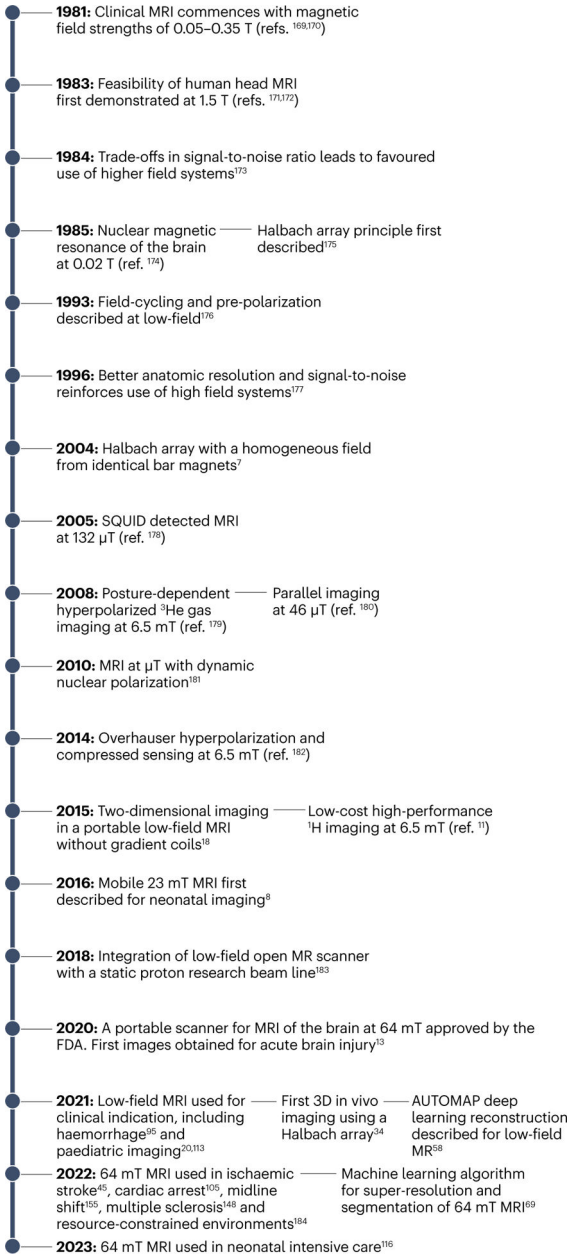

Fig. 3 |. The evolution of LF-MR neuroimaging.

In the early 1980s, MR magnets operated in the low-field (LF) range. The inherent reduced signal-to-noise ratio facilitated development of higher-field systems, with the perception in the scientific community that higher static field strength equated to better performance. Despite several advances in the 1990s, the turn of the millennium saw a renaissance of LF-MRI. The first FDA-approved device was deployed in 2020 and, since 2021, LF-MRI at 0.064 T has been investigated in a range of conditions and environments. As LF-MRI continues to evolve, bioengineers will play an increasing role in its future. AUTOMAP, end-to-end deep neural network approach; SQUID, superconducting quantum interference device[169–184].